A Nano-opto-mechanical Pressure Mapping Sensor via Bragg Structure Waveguide for Biomedical Sensing

Xin Zhao
College of Physical Science and Technology, Sichuan University, China
*Institute of Microelectronics, A*STAR (Agency for Science, Technology and Research), 11 Science Park Road, Science Park II, Singapore117685, Singapore*
School of Electrical & Electronic Engineering, Nanyang Technological University, Singapore 639798, Singapore

Keywords: Nano-electro-mechanical Systems, Bragg Structure Waveguide, Mapping Sensor.

Abstract: This paper reports a nano-opto-mechanical mapping sensor based on Bragg structure waveguide. The pressure is measured by monitoring the output spectrum shift which is induced via mechanical deformation of the period of the Bragg structure. In experiments, it measures that the shifting of the output spectra linearly red shift under different position of the Bragg structure when the pressure is increasing. Compared with traditional optical mapping sensor based on Mach-Zehnderinterferometer, the nano-opto-mechanical mapping sensor has merits such as high sensitivity and fine resolution which are 1.55pm/kPa and 1.29kPa, respectively. The nano-opto-mechanical mapping sensor has potential applications such as highly accurate measurement of pressure waves, mass sensors array and bio-medical sensors.

1 INTRODUCTION

Optical pressure sensors have advantages such as immunity to electromagnetic interference (EMI), lightweight, small device scale, high sensitivity, and ease in signal transmission, etc, compared with electrical pressure sensors which are sensitive to almost everything such as light, temperature, pressure, electromagnetic (EM) field and humidity. During the past thirty years, various ideas have been developed based on optical pressure sensors. Most of the optical pressure sensors are based on either optical fibers, or single waveguide. However, optical fibers pressure sensor occupy large area, the fibers are not easy to be integrated with silicon based photonic chips and cannot be fabricated using standard complementary metal–oxide–semiconductor (CMOS) technology. In MZI structure pressure sensor, the waveguide branches or 3-dB directionalcouplers making the optical devices long. The single waveguide pressure sensors need additional input and output polarizers to form TM-TE intermodal interference in a single-mode waveguide. Single waveguide structure pressure sensor as well as MZI structure pressure sensors suffer from nonlinear optical intensity output. Pressure sensors have been fabricated using many different technologies such as glass, piezoelectric quartz crystals, II–VI compound photoconductors, and metal diaphragm. However silicon based pressure sensors are most likely to be commercialized due to their feasibility in mass production and low cost. Although the introduction of silicon cannot guarantee the improvements of the performances, it definitely has great advantage in producing micro-scaled or even nano-scale pressure sensors which can be integrated in photonic circuits. In this paper, the Bragg structure in silicon waveguide is induced in the pressure sensor. A novel nano-opto-mechanical pressure sensor based on Bragg structure waveguide is proposed to provide a reliable optical pressure sensor with high sensitivity, good linearity of the output, CMOS compatibility and ease in constructing sensors array.

2 DESIGN AND THEORETICAL ANALYSIS

The design of the proposed pressure sensor is shown in Fig. 1(a). The pressure sensor consists of a 820 × 820 μm^2 diaphragm, five waveguides with Bragg structure. The coordinate (0,0) is set at the center of the diaphragm with the unit length as 1 μm. The

Zhao X..
A Nano-opto-mechanical Pressure Mapping Sensor via Bragg Structure Waveguide for Biomedical Sensing.
DOI: 10.5220/0005274101380143
In *Proceedings of the International Conference on Biomedical Electronics and Devices* (BIODEVICES-2015), pages 138-143
ISBN: 978-989-758-071-0

centers of the Bragg structures are located at (0, 0), (45, 45), (-45, -45), (84, -84), (-84, 84), respectively. The period of the Bragg structure *a* is 0.6 µm. The diameter of the hole *d* is 0.3 µm as shown in Fig. 1(b). The diaphragm consists of SiO_2 layer and Si layer with thickness of 2 µm and 18 µm, respectively as shown in Fig.1(c).

The pressure applied to the diaphragm causes the shear stress displacement. The shear stress displacement results in the change of the period of the Bragg structure Δa as shown in the Fig 1(b). The Δa influences the effective refractive index of the Bragg structure Δn_{eff}. Both the Δa and the Δn_{eff} results in the resonant wavelength shift of the Bragg structure $\Delta\lambda$. The $\Delta\lambda$ could be read out from the output spectrum of the waveguide. The pressure applied to the diaphragm is detected by the $\Delta\lambda$.

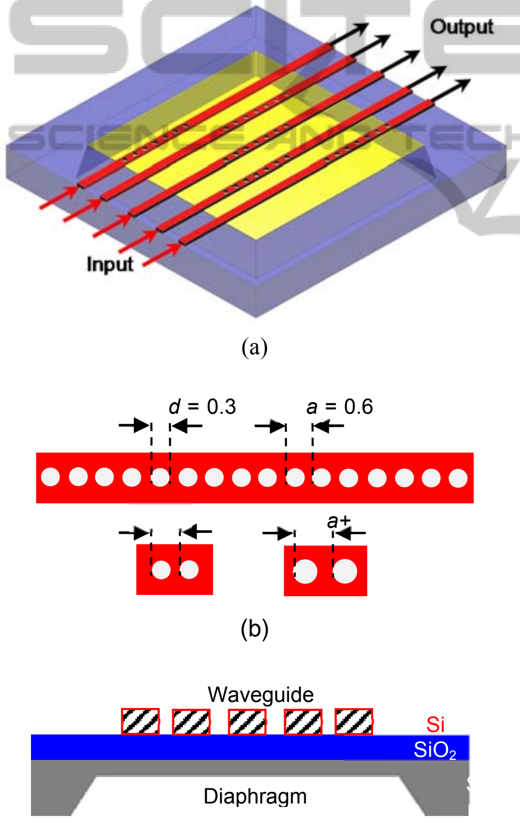

(a)

(b)

(c)

Figure 1: (a) Schematic of the nano-opto-mechanical pressure sensor, (b) Bragg structure, and (c) cross-section of the pressure sensor.

2.1 Mechanical Design

The deformation of the diaphragm in x, y and z direction is necessary to calculate the period change of the Bragg structure Δa due to the applied pressure on the diaphragm. The deflection of diaphragm along z- direction *w*, the displacement along x- direction u, and displacement along y- direction *v* are the solution of the differential equation of diaphragm are expressed as,

$$\nabla^4 w-\gamma^2\nabla^2 w=\frac{P}{D_{eq}} \quad (1a)$$

$$\gamma^2=\frac{12}{h^2}\left[\frac{\partial u}{\partial x}+\frac{\partial v}{\partial x}+\frac{1}{2}\left(\frac{\partial w}{\partial x}\right)^2+\frac{1}{2}\left(\frac{\partial w}{\partial y}\right)^2\right] \quad (1b)$$

$$D_{eq}=\sum_{i=1}^{n}\frac{E_i h_i^3}{12\left(1-v_i^2\right)} \quad (1c)$$

where γ is the constant of integration, P is the uniform pressure, D_{eq} is the bending rigidity of the equivalent single-layer, *n* is the number of the layer, E_i is the Young's modulus of the i layer material, i equate 1 or 2 in our design for SiO_2 layer or Si layer, h_i is the thickness of i layer, v_i is Poisson's ratio of i layer, h is the thickness of the whole diaphragm.

Finite Element Method is used to calculate the membrane deformation. Fig 2(a) shows the deflection of diaphragm *w* along z-direction, when the P is 60 kPa. Fig2(b) illustrates the displacement along x direction *u*. The P is 12 kPa, 42 kPa, and 60 kPa, respectively. The diaphragm position is along the diagonal of the diaphragm plane. Fig. 2(c) shows the relation between the change rate of *u* and the position of the diaphragm along diagonal of the diaphragm. The change rate of *u* reaches the maximum 58.9×10^{-6} when the position of the diaphragm is (0,0). The P is 12 kPa, 42 kPa, and 60 kPa, respectively. The thickness of the waveguide is 0.22 µm, which is much less than 20 µm. Therefore, the shear stress of the diaphragm could influence both the top and bottom edges of the air holes in the Bragg structure. In this condition, the value of Δu between edges of the two adjacent air holes equal to Δa along x direction.

The relation between the Δa and P is shown in the Fig 2(d). The Δa is proportional linearly to the change of pressure ΔP for different position of the Bragg structure.

$$\Delta a = C_1 P \quad (2)$$

where C_1 are 0.592 pm/kPa, 0.539 pm/kPa and 0.412 pm/kPa, respectively, when the centre position of the Bragg structure are (0, 0), (45, 45), and (-84, 84) as shown in Fig. 2 (d).

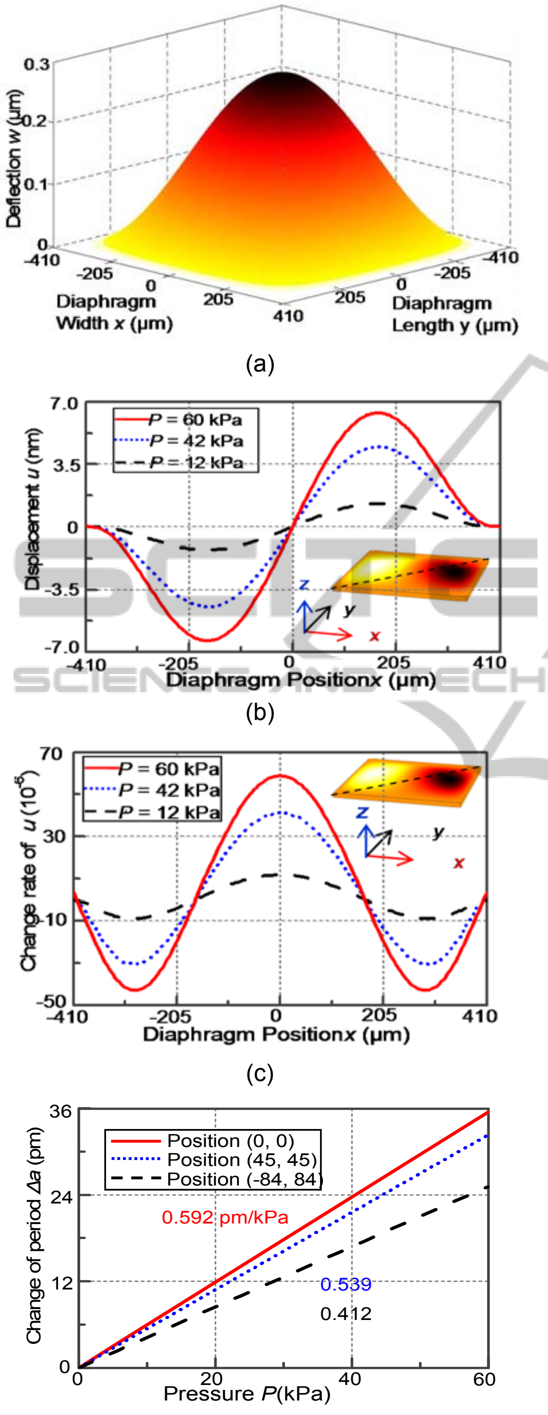

(a)

(b)

(c)

(d)

Figure 2: (a) The deflection along z-direction, and (b) the displacement along x-direction of the diaphragm when the applied pressure is 60 kPa. The different y value are 0 μm, 45 μm, and 84 μm, respectively. (c) The change rate of displacement along x-direction (d) The period change of Bragg structure Δa, when the centre position of the Bragg structures are (0, 0), (45, 45), and (-84, 84). The applied pressure is from 0 to 60kPa.

2.2 Optical Design

The pressure applied on the diaphragm can be read out by the wavelength shift. The resonant wavelength λ can be inferred from the following equation based on the coupling condition of the Bragg waveguide,

$$2n_{eff}a = m\lambda \tag{3}$$

where m is the mode number. Calculated by the Finite-difference-time-domain (FDTD) method, n_{eff} is 2.6553, when a is 0.6 μm, and pressure is zero. The resonant wavelength shift Δλ as a function of Δn_{eff} and Δa can be written as

$$\Delta\lambda = \frac{2\left(n_{eff}+\Delta n_{eff}\right)\left(a+\Delta a\right)}{m} - \frac{2n_{eff}a}{m} \tag{4}$$

The Δa causes the change of the horizontal hole radius ratio to the lattice period r/a which results in the change of the Bragg structure Δn_{eff}. Calculated by Finite Element Method, The relation between the Δn_{eff} and Δa can be written as:

$$\Delta n_{eff} = C_2\Delta a \tag{5}$$

where C_2 are -0.071×10^{-6} /pm, -0.064×10^{-6} /pm and -0.060×10^{-6} /pm, respectively, when the centre position of the Bragg structure are (0, 0), (45, 45), and (-84, 84) as shown in Fig. 3. The relation between the Δn_{eff} and Δa is linear.

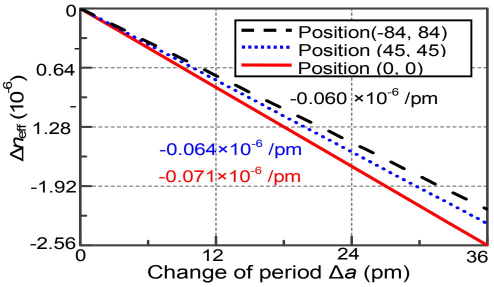

Figure 3: Change of effective refractive index Δn_{eff} due to the change of period Δa.

The Eq. (4) can be expressed as:

$$\Delta\lambda = \frac{2\left(n_{eff}\Delta a + \Delta n_{eff}a + \Delta n_{eff}\Delta a\right)}{m} \approx \frac{2\left(n_{eff}\Delta a + \Delta n_{eff}a\right)}{m} \tag{6}$$

$\Delta n_{eff}\Delta a$ is 9.2×10^{-17} which can be ignored. The relationship between Δλ and P is obtained by substituting Eq. (2) and Eq. (5) into Eq. (6).

$$\Delta\lambda = \frac{2\left[n_{eff}C_1 + C_1C_2a\right]P}{m} = C_3P \tag{7}$$

where $C_3 = \Delta\lambda/P$ is the sensitivity of the nano-opto-mechanical pressure sensor, m is 2. Here, transverse electric (TE) and transverse magnetic (TM) mode is defined as the propagating mode with the electrical field parallel and perpendicular to the diaphragm plane, respectively. Only TE mode polarization exists in the ring resonator and the bus waveguide since the thickness of the waveguide is designed to be smaller than the cutoff width of TM mode. Therefore, n_{eff} refers to the effective index of TE mode only. The variation of n_{eff} caused by the photo-elastic effect is approximately 10^{-7} which has trivial effect, compared with the change of the period, on $\Delta\lambda$.

3 EXPERIMENTAL RESULTS AND DISCUSSIONS

The SEM images of the fabricated nano-opto-mechanical pressure sensor are shown in Fig. 4. All structures are fabricated on a standard silicon-on-insulator (SOI) wafer with a silicon structure layer of 220 nm. The thickness of silicon dioxide (SiO_2) layer and back side substrate is 2 µm and 720 µm, respectively. The waveguide and the Bragg structure are patterned by deep UV lithography, followed by Reactive Ion Etching to transfer the photo resist pattern into the silicon structure layer. Potassium hydroxide (KOH) wet etching is used to form the backside open of diaphragm with thickness of 20 µm. For comparison, five different parameters are used for the fabrication of the nano-opto-mechanical pressure sensors which are the center position of the Bragg structure: (0, 0), (45, 45), (-45, -45), (-84, 84), and (84, -84).

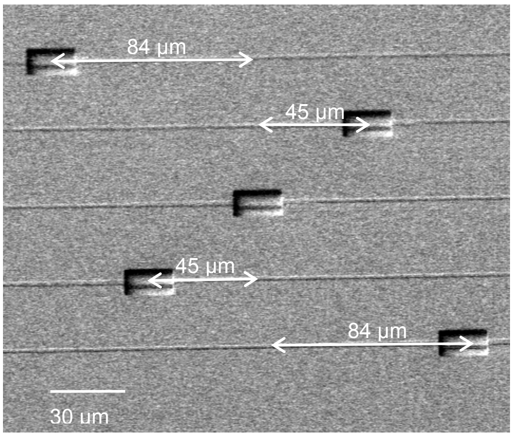

(a)

Figure 4: SEM images of (a) pressure sensor, and (b) zoom view of the Bragg structure.

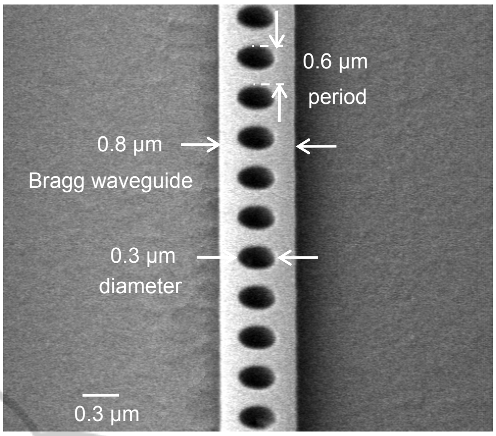

(b)

Figure 4: SEM images of (a) pressure sensor, and (b) zoom view of the Bragg structure (cont.).

Fig. 4(a) shows the overview of the pressure sensor with a footprint of 1.8 mm × 1.8 mm which is the same size as the etching window of backside open. Fig. 4(b) shows the zoom view of the the Bragg structure of the waveguide. The cross-section of the Bragg structure is 800 nm × 220 nm. The period of the Bragg structure is 0.6 µm. The diameter of the air hole is 0.3 µm. These nano-scaled structures are used to keep the single-mode propagation of the light.

The nano-opto-mechanical pressure sensor is tested by using the fiber-to-chip alignment system PS-1000 from SURUGA SEIKI CO.,LTD. The incident broadband source is Amplified Spontaneous Emission which has 8-mW output power over the spectrum ranging from 1570 nm to 1608 nm. The light is input from one end of the bus waveguide and monitored from the other end using an optical spectrum analyzer AP2052A from Apex Technologies.

The output spectra of the nano-opto-mechanical pressure sensor at different pressures applied to the diaphragm is shown in Fig. 5(a). Here, the diaphragm thickness is 20 µm. The measured propagation loss of the waveguide is approximately 1.9 dB/cm. The resonance dip wavelength red shifts from 1593.194 nm to 1593.287 nm when the pressure on the diaphragm is increasing from 0 kPa to 60 kPa. The quality factor of the resonance peak is around 8.92×10^3 which is slightly broadened because of the deformation of the ring resonator and the bus waveguide induced by the pressure applied to the diaphragm. Fig. 5(b) shows the wavelength shift $\Delta\lambda$ versus pressure P measured from three different samples. The symbols and the lines

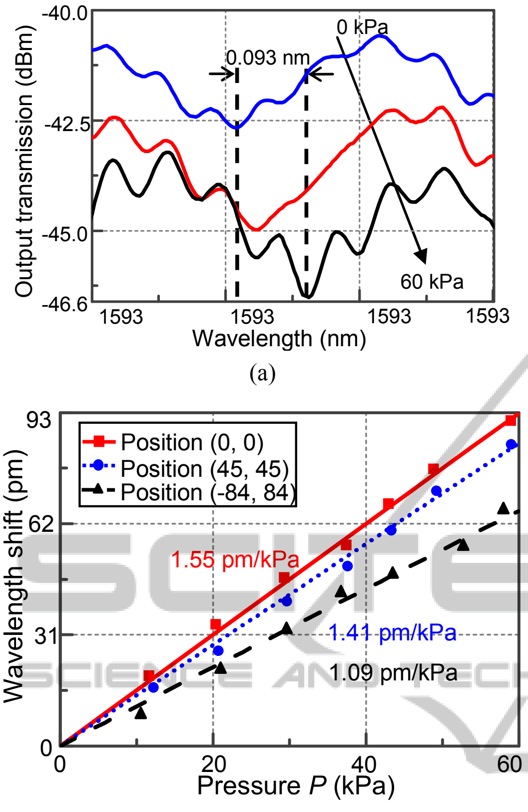

(a)

(b)

Figure 5: Transmission spectra at various applied pressures on the diaphragm. The centre position of the Bragg structures are (0, 0), and (b) wavelength shift versus the pressure when the centre position of the Bragg structure are (0, 0), (45, 45), and (-84, 84).

represent the measured and simulated results, respectively. The solid, dotted and dashed line show the $\Delta\lambda$ as the function of P when the center position of the Bragg structure is (0, 0), (45, 45), and (-84, 84), respectively which shows a good linearity between the output of the pressure sensor and the measured pressure. The slopes of the lines $C_3 = \Delta\lambda/P$ is equal to the sensitivity of the nano-opto-mechanical pressure sensor. C_3 is 1.55×10^{-3} nm/kPa, when the center position of the Bragg structure is (0, 0) which is at least 1.42 times larger than that of the (-84, 84). The resolution of the nano-opto-mechanical pressure sensor is limited by the resolution of the optical spectrum analyzer used in the experiment. The optical spectrum analyzer allows for a spectral resolution of approximately 2 pm. Consequently, the pressure resolution is 1.29 kPa which can be obtained by the Eq. (7).

4 CONCLUSIONS

In summary, a highly sensitive nano-opto-mechanical pressure mapping sensor based on Bragg structure is designed, fabricated and characterized for pressures ranging from 0 kPa to 60 kPa. The sensitivity as high as 1.55 pm/kPa has been experimentally achieved which is in good agreement with numerical prediction. The pressure sensor structure make it possible to detect the shear stress displacement distribution in highly accurate measurement with low-cost advantages. The characteristics indicate potential for various applications such as mass sensor, bio-medical sensors and optical integrated circuits etc.

REFERENCES

D. Donlagic and E. Cibula, 2005.All-fiber high-sensitivity pressure sensor with SiO2 diaphragm. *Opt. Lett.*

G. T. Kanellos, G. Papaioannou, D.Tsiokos, C. Mitrogiannis, G. Nianios and N. Pleros, 2010.Two dimensional polymer-embedded quasi-distributed FBG pressure sensor for biomedical applications. *Opti. Express.*

Y. C. Chao, W. J. Lai, C.Y. Chen, H. F. Meng, and H W Zan, 2009."Low voltage active pressure sensor based on polymer space-change-limited transitor. *Appl. Phys. Lett.*

M. Esashi, H. Komatsu, and T. Matsuo, 1983.Biomedical pressure sensor using buried piezoresistors. *Sens. Actuators A.*

C. S. Sander, J. W. Knutt and J. D. Meindl, 1980.A monolithic capacitive pressure sensor with pulse-period output.*IEEE Trans. Electron Devices.*

D. D. Bruyker, and R. Puers, 2000.Thermostatic control for temperature compensation of a silicon pressure sensor.*Sens. Actuators A.*

M. C. Oh, J. W. Kim, K. J. Kim, and S. S. Lee, 2009.Optical pressure sensors based on vertical directional coupling with flexible polymer waveguides. *IEEE Photonics Technol. Lett.*

M. Shimada, Y. Kinefuchi, and K. Takahashi, 2008.Sleeve-type ultra miniature optical fiber pressure sensor fabricated by DRIE. *IEEE Sensors J.*

Y. Zhu and A. Wang, 2005.Miniature fiber-optic pressure sensor, *IEEE Photon. Technol. Lett.*

B.J. Luff, J.S.Wilkinson, J. Piehler, U. Hollenbach, J. Ingenhoff, N. Fabricius, 1998.Integrated optical Mach–Zehnder biosensor. *J. Light. Technol.*

M. Ohkawa, M. Izutsu, and T. Sueta. 1989.Integrated optic pressure sensor on silicon substrate, Appl. Opt.

N. Pelletier, B. Bêche, N. Tahani, J. Zyss, L. Camberlein, and E.Gaviot, 2007.SU-8 waveguiding interferometric micro-sensor for gage pressure measurement. *Sens. Actuators A.*

Y. S. Hsu, L. Wang, W.-F. Liu, and Y. J. Chiang, 2006.Temperature compensation of optical fiber Bragg grating pressure sensor. *IEEE Photon.Technol. Lett.*

T. H. Ning,1997.Trends in CMOS technology and application development,Mater. Chem. Phys. W. P. Eaton, and J. H. Smith.Micromachined pressure sensors: review and recent developments. *Smart Mater. Struct.*

X. P. Wu, M. F. Hu, J. Y. Shen and Q. H. Ma, 1993.A miniature piezoresistive catheter pressure sensor. *Sens. Actuators A.*

C. T. Peng, J. C. Lin, C. T. Lin and K. Ning. Chiang, 2005.Performance and package effect of a novel piezoresisitive pressure sensor fabricated by front-side etching technology. *Sens. Actuators A.*

M. T. C. Silva, and S. K. Manfrin, 1995.Silicon integrated optical pressure sensor based on distributed Bragg reflector structure. *SPIE.*

H. M. Berger, 1954.A new approach to the analysis of large deflections of plates.

K. Okamoto, 2006.Fundamentals of optical waveguides. Second edition.